

Molecular BioSystems

Accepted Manuscript



This is an *Accepted Manuscript*, which has been through the Royal Society of Chemistry peer review process and has been accepted for publication.

Accepted Manuscripts are published online shortly after acceptance, before technical editing, formatting and proof reading. Using this free service, authors can make their results available to the community, in citable form, before we publish the edited article. We will replace this *Accepted Manuscript* with the edited and formatted *Advance Article* as soon as it is available.

You can find more information about *Accepted Manuscripts* in the [Information for Authors](#).

Please note that technical editing may introduce minor changes to the text and/or graphics, which may alter content. The journal's standard [Terms & Conditions](#) and the [Ethical guidelines](#) still apply. In no event shall the Royal Society of Chemistry be held responsible for any errors or omissions in this *Accepted Manuscript* or any consequences arising from the use of any information it contains.



www.rsc.org/molecularbiosystems

Cite this: DOI: 10.1039/c0xx00000x

www.rsc.org/xxxxxx

ARTICLE TYPE

An orphan two-component response regulator Slr1588 involves salt tolerance by directly regulating synthesis of compatible solutes in photosynthetic *Synechocystis* sp. PCC 6803

5 Lei Chen^{1,2,3}, Lina Wu^{1,2,3}, Ye Zhu^{1,2,3}, Zhongdi Song^{1,2,3}, Jiangxin Wang^{1,2,3}, Weiwen Zhang^{1,2,3*}

¹ Laboratory of Synthetic Microbiology, School of Chemical Engineering & Technology, Tianjin University, Tianjin 300072, P.R. China

² Key Laboratory of Systems Bioengineering, Ministry of Education of China, Tianjin 300072, P.R. China

³ Collaborative Innovation Center of Chemical Science and Engineering, Tianjin, P.R. China

10

* To whom all correspondence should be addressed:

Prof. Dr. Weiwen Zhang

Laboratory of Synthetic Microbiology

School of Chemical Engineering & Technology

15 Tianjin University, Tianjin 300072

People's Republic of China

Tel : 0086-22-2740-6394; Fax : 0086-22-27406364; Email: wwzhang8@tju.edu.cn

Abstract

20 We report here the characterization of a novel orphan response regulator Slr1588 directly involved in synthesis and transport of compatible solutes against salt stress. In the $\Delta slr1588$ mutant, salt tolerance was found decreased by 2-3 folds. Using a high performance Q-EXACTIVE hybrid quadrupole-Orbitrap mass spectrometer, we found that proteins involved in synthesis and transport of glucosylglycerol, a key compatible solute, were up-regulated in the $\Delta slr1588$ mutant grown under 4.0% NaCl, suggesting Slr1588 might function as a repressor for glucosylglycerol metabolism. The functional assignment was further confirmed by electrophoretic mobility shift assay (EMSA) showing the purified his-tagged Slr1588 could bound *in vitro* directly to the upstream regions of *slr1566* (*ggpS*) genes required for glucosylglycerol biosynthesis. In addition, quantitative proteomic analysis showed that biosynthesis of another key compatible solute in *Synechocystis*, sucrose, was also up-regulated in the $\Delta slr1588$ mutant under 4.0% NaCl, and EMSA showed that the purified his-tagged Slr1588 bound *in vitro* directly to the upstream regions of *slr1045* (*spsA*) gene required for sucrose biosynthesis. Moreover, proteomic analysis showed that 113 and 127 unique proteins were up- and down-regulated in the $\Delta slr1588$ mutant grown under 4.0% NaCl, respectively. Notably, a dozen transporter genes were down-regulated in the $\Delta slr1588$ mutant under salt stress. The study revealed a novel salt-tolerant regulatory mechanism mediated by Slr1588, and also provided a proteomic description of the possible Slr1588 regulon in *Synechocystis*.

Key words: Response regulator, Proteomics, Salt, *Synechocystis*

Introduction

Microbes must modulate their metabolic activities in response to changing environments. One of the predominant signal transduction mechanisms employed by microbes is the histidine-aspartate phosphorelay system, also known as two-component signal transduction systems (TCSTSs), which is arguably the most widespread mechanism of signal transduction that bacteria use to sense and respond to their environments [1]. TCSTS typically consists of a sensor histidine kinase and a response regulator. In most cases, coding genes for sensor kinase and its cognate response regulator are clustered together in chromosome in order to achieve highly coordinated and efficient signal transfer; however, it is also commonly observed that histidine kinase or response regulator is separately located, as an “orphan” gene, from its cognate partner in chromosomes [1,2]. In the past decades, significant researches have been conducted to determine the possible regulatory functions of various TCSTSs, and the results showed that TCSTSs were involved in regulation of a very wide variety of cellular responses, including chemotaxis, cellular differentiation, sporulation, antibiotic production, pathogenicity, osmoregulation, photosynthesis, circadian timing and many others in a number of different bacteria [3-6].

Changing concentration of salt is one of the most common abiotic stress factors on the earth [7]. It thus came no surprise that TCSTSs have been identified involved in the adaptation to salt concentration in many bacteria, and some of these TCSTS systems, such as DegS-DegU system in *Bacillus subtilis* [8], NtrY/NtrX system in *Rhizobium tropici* [9], KdpE/RsbQ system in *Listeria monocytogenes* [10], a response regulator in a halophilic *Chromohalobacter salexigens* [11], CpxR/OmpR, KdpD/KdpE and OmpR-EnvZ systems in *Escherichia coli* [12-15], have been well characterized.

As the important primary producers of fixed carbon budget in many terrestrial and marine environments, photosynthetic cyanobacteria are responsible for at least 20% of global carbon fixation [16]. Due to their significant ecological roles, effects of high and changing salt concentration on cyanobacteria, especially on the model species *Synechocystis* sp. PCC 6803 (hereafter *Synechocystis*), have been intensively studied [7]. The results showed that cyanobacterial cells went through five sequential acclimation phases, each with their very unique metabolic and morphological changes, in order to achieve a fully salt-acclimated status [17-22]. To execute such global and sequential cellular responses timely and accurately, sophisticated regulatory mechanism must be involved. In an early study, Schwartz *et al.* (1998) showed that an *orrA* gene whose predicted product showed sequence similarity to response regulators from TCSTSs was involved in regulation of salt-induced genes in *Anabaena* sp. PCC 7120 [23]. Marin *et al.* (2005) applied a genome-wide microarray to screen a library of strains with mutations in all 43 histidine kinases of *Synechocystis*, the results

suggested that four histidine kinases, namely, Hik16, Hik33, Hik34, and Hik41, perceived and transduced salt signals, and together they regulated the expression of approximately 20% of the salt-inducible genes. However, remaining 80% of the salt-inducible genes was unaffected by mutations in any of the histidine kinases, suggesting that additional sensory mechanisms might operate in the perception of salt stress [24]. Shoumskaya *et al.* (2005) screened a gene knock-out library of response regulators (Rres) of *Synechocystis* by RNA slot-blot hybridization and with a genome-wide DNA microarray and identified three Hik-Rre systems, namely, Hik33-Rre31, Hik10-Rre3, and Hik16-Hik41-Rre17, as well as another system that included Rre1, that were involved in perception of salt stress and transduction of the signal [25]. While these studies clearly demonstrated that TCSTSs are one of the primary signal transduction mechanisms involved in salt responses in *Synechocystis*, the results also indicated that additional TCSTS genes might be involved in salt responses [24].

Our laboratory has been focusing on the biotechnological application of *Synechocystis* for producing various biofuels and fine chemical products [26,27]; towards this goal, robust and stress-tolerant *Synechocystis* chassis need to be engineered [28-31]. It has been recently proposed that engineering regulatory machinery in cells could be a very efficient way to increase stress tolerance since the approach could generate more global changes that are not readily manipulated by traditional methods of targeting some number of metabolic genes [32,33]. To uncover TCSTSs that may be involved in response to various stresses, we screened a library of gene knockout mutants for all 44 *Synechocystis* response regulators (among which 2 mutants were only partially segregated), and the efforts led to identification of an orphan response regulator Slr1588 involved in salt tolerance. To further determine the response network related to the gene, we then applied Q Exactive high-performance mass spectrometer for a quantitative iTRAQ-LC-MS/MS based proteomics, along with electrophoretic mobility shift assays (EMSAs) to identify the possible gene targets downstream of Slr1588. The results showed that Slr1588 may be able to bind directly to the upstream regions of genes required for the biosynthesis of glucosylglycerol and sucrose, and may thus function as a repressor for both glucosylglycerol and sucrose metabolism. The study provided novel information regarding the salt tolerance regulation in *Synechocystis*.

Experimental

Bacterial growth conditions

Synechocystis sp. PCC 6803 and the TCSTSs knockout mutants including $\Delta slr1588$ constructed in this study were grown in BG11 medium (pH 7.5) under a light intensity of approximately 50 $\mu\text{mol photons m}^{-2} \text{s}^{-1}$ in an illuminating shaker of 130 rpm at 30°C (HNY-211B Illuminating Shaker, Honour, China) [29,30]. Cell density was measured on a UV-1750 spectrophotometer (Shimadzu, Japan). For control

Cite this: DOI: 10.1039/c0xx00000x

www.rsc.org/xxxxxx

ARTICLE TYPE

160 growth and salt (NaCl, 4.0%, w/v) treatment in liquid
medium, 10 mL fresh cells at OD₇₃₀ of 0.5 collected
by centrifugation and then were inoculated into 50 mL
BG11 liquid medium in a 250-mL flask. For growth
on BG11 agar plate, 3 µL of fresh cells at OD₇₃₀ of 0.5
165 and its series of ten-fold dilutions were inoculated
onto normal BG11 agar plate or BG11 agar plate
supplemented with 2.5% or 3.0% NaCl, and then
incubated in an illuminating incubator at 30°C (SPX-
250B-G Illuminating Incubator, Boxun, China) for up
170 to 4 days. Growth experiments were repeated at least
three times to confirm the growth patterns. Cells for
proteomics analysis were collected at 48 h of the
exponential phase by centrifugation at 8,000 x g for 10
min at 4°C.

Construction and analysis of knockout mutants

175 A fusion PCR based method was employed for the
construction of gene knockout fragments [34]. Briefly,
for the gene target selected, three sets of primers were
designed to amplify a linear DNA fragment containing
the kanamycin resistance cassette (amplified from a
180 plasmid pET30a(+)) with two flanking arms of DNA
upstream and downstream of the targeted gene. The
linear fused PCR amplicon was used directly for
transformation into *Synechocystis* by natural
transformation. The kanamycin-resistant transformants
185 were obtained and passed several times on fresh BG11
plates supplemented with 10 µg/mL kanamycin to
achieve complete chromosome segregation. The
successful knockout mutant was confirmed by PCR
and sequencing analysis. PCR primers used for mutant
190 construction and validation were listed in **Suppl.**
Table S1.

Proteomics analysis

195 *i) Protein preparation and digestion:* for each sample,
10 mg of cells were frozen by liquid nitrogen
immediately after centrifugation and washed with
phosphate buffer (pH 7.2). The cells were broken with
sonication cracking at low temperature. Cell pellets
200 were then resuspended in a lysis buffer (8 M urea, 4%
CHAPS, 40 mM Tris-HCl), with 1 mM
phenylmethanesulfonyl fluoride (PMSF) and 2 mM
ethylenediaminetetraacetic acid (EDTA) (final
concentration). After 5 min of vigorously vortex,
205 dithiothreitol (DTT) was also added to a final
concentration of 10 mM. After mix, the sample were
centrifuged for 20 min at 20,000 x g, and the
supernatant was mixed well with ice-cold acetone (1:4,
v/v) with 30 mM DTT. After repeating this step twice,
210 supernatants were combined and precipitated at -20°C
overnight, and stored at -80°C prior to sample cleanup
if not for immediate use. For digestion, protein pellet
from previous step was resuspended in digestion

215 buffer (100 mM triethylammonium bicarbonate TEAB,
0.05% w/v sodium dodecyl sulfate, SDS) to a final
concentration of 1 mg/mL [total protein measured by
bicinchonic acid assay (Sigma, St. Louis, MO)]. Equal
aliquots (500 µg) from each lysate were then digested
with trypsin overnight at 37°C (Sigma; 1:40 w/w
220 added at 0 and 2 h) and lyophilized; *ii) iTRAQ*
Labeling: the iTRAQ labeling of peptide samples
derived from the wild type control and the gene
knockout mutant samples were performed using
iTRAQ Reagent 8-plex kit (Applied Biosystems,
225 Foster City, CA) according to the manufacturer's
protocol. Four samples (two biological replicates for
the wild type control and two biological replicates for
the $\Delta slr1588$ knockout mutant, respectively) were
iTRAQ labeled. The peptides labeled with respective
230 isobaric tags, incubated for 2 h and vacuum
centrifuged to dryness. The labeled control and the
mutant replicate samples were 1:1 pooled, and
generating four combinations of samples, which were
reconstituted in Buffer A (10 mM KH₂PO₄, 25%
235 acetonitrile, pH 2.85); *iii) SCX separation:* The
iTRAQ labeled peptides were fractionated using
UltremexSCX column (250 x 4.6 mm, 5 µm particle
size, 200 Å pore size) of Shimadzu LC-20AB HPLC
system (Shimadzu, Japan) at flow rate 1.0 mL min⁻¹.
240 The 22 min HPLC gradient consisted of 100% buffer
A (25 mM NaH₂PO₄ in 25% acetonitrile, pH 2.7) for
10 min, 5-35% buffer B (25 mM NaH₂PO₄, 1M KCl
in 25% acetonitrile, pH 2.7) for 11 min, followed by
35-80% buffer B for 1 min. The chromatograms were
245 recorded at 214 nm. The collected 20 fractions were
desalted with Sep-Pak® Vac C18 cartridges (Waters,
Milford, Massachusetts), and concentrated to dryness
using vacuum centrifuge. *iv) LC-MS/MS proteomic*
analysis: The dried fractions were reconstituted in
250 Buffer C (5% acetonitrile and 0.1% formic acid) for
the LC-MS/MS analysis. Approximately 4 g of
proteins from each fraction were subjected to HPLC
separation using Shimadzu LC-20AD HPLC system
(Shimadzu, Japan) at flow rate 300 nL min⁻¹. The 50
255 min HPLC gradient consisted of 2-35% Buffer D (95%
acetonitrile, 0.1% formic acid) at 300 nL/min for 40
min, followed by 35-80% buffer D for 5 min and 80%
buffer D for 4 min, and then eluted by buffer C for 1
min. The mass spectroscopy analysis was performed
260 using an Q-EXACTIVE hybrid quadrupole-Orbitrap
mass spectrometer (ThermoFisher Scientific, San Jose,
CA, USA) [35,36]. The Q Exactive instrument was
operated in the data dependent mode to automatically
switch between full scan MS and MS/MS acquisition.
265 Survey full scan MS spectra (m/z 300–1750) were
acquired in the Orbitrap with 70,000 resolution (m/z
200). Dynamic exclusion was set to 30 s. The 12 most
intense multiply charged ions ($z \geq 2$) were

sequentially isolated and fragmented in the octopole collision cell by higher-energy collisional dissociation (HCD) with a fixed injection time of 60 ms and 17000 resolution for the fast scanning method. The peak areas of the iTRAQ reporter ions reflect the relative abundance of the proteins in the samples. For peptide identification, Q-Exactive mass spectrometer used in this study has high mass accuracy (less than 2 ppm); *v*) *Proteomic data analysis*: the MS data were processed using Proteome Discoverer software (Version 1.2.0.208) (Thermo Scientific) to generating peak list. The default parameters of Proteome Discoverer software (Version 1.2.0.208) were used. The data acquisition was performed with Analyst QS 2.0 software (Applied Biosystems/MDS SCIEX). Protein identification and quantification were performed using Mascot 2.3.02 (Matrix Science, London, United Kingdom). The key parameters of peptide identification included: Fragment Mass Tolerance, ± 15 ppm; Mass Values, Monoisotopic; Variable modifications, Gln->pyro-Glu (N-term Q), Oxidation (M), iTRAQ8plex (Y); Peptide Mass Tolerance, ± 0.02 Da; Fixed modifications, Carbamidomethyl (C), iTRAQ8plex (N-term), iTRAQ8plex (K); and default for other parameters. For iTRAQ quantification, the peptide for quantification was automatically selected by the algorithm to calculate the reporter peak area, error factor (EF) and *p*-value (default parameters in Mascot Software package). Genome sequence and annotation information of *Synechocystis* sp. PCC 6803 were downloaded from NCBI, the Comprehensive Microbial Resource (CMR) of TIGR (<http://www.tigr.org/CMR>) and CyanoBase (<http://genome.microbedb.jp/cyanobase/>) [37]. Proteins with 1.5 fold or more change between the $\Delta slr1588$ mutant and the control samples and *p*-value of statistical evaluation less than 0.05 were determined as differentially expressed proteins. The quantitation was performed at the peptide level by following the procedures described in http://www.matrixscience.com/help/quant_statistics_help.html.

Quantitative Real-Time Reverse Transcription-PCR analysis

The identical cell samples used for protein isolation as described above were used for RT-qPCR analysis as described previously [31]. The *rnpB* gene (*6803s01*) encoding RNase P subunit B was used as an internal control [38]. Three technical replicates were performed for each gene. Data analysis was carried out using the StepOnePlus analytical software (Applied Biosystems, Foster City, CA). The gene ID and their related primer sequences used for real-time RT-PCR analysis were listed in **Suppl. Table S1**.

Overexpression and purification of His₆-Slr1588 protein

The *slr1588* gene of *Synechocystis* was amplified using primer pairs to introduce appropriate 5' extensions before its ATG initiation codon and behind

its stop codon (**Suppl. Table S1**). The resulting target fragment was treated with T4 DNA Polymerase in the presence of dATP to generate specific vector-complementary overhangs, and then annealed to pET46 Ek/LIC vector treated with the same enzymes, generating the recombinant plasmid pET46-1588. After confirmation by DNA sequencing, the pET46-1588 plasmid was introduced into *E. coli* BL21 (DE3) for protein expression. *E. coli* BL21 (DE3) harboring pET46-1588 was grown in 350 mL LB with 100 μ g/mL ampicillin at 37°C to an OD₆₀₀ of ~ 0.6 . The cultures were then induced by adding isopropyl β -D-1-thiogalactopyranoside (IPTG) at a final concentration of 0.2 mM and incubating further at 18°C overnight. For the purification of His₆-Slr1588, the cells were harvested by centrifugation at 5000 \times g, 4°C for 10 min, washed twice with binding buffer [50 mM Tris-HCl, 500 mM NaCl, 10 mM imidazole, 10% glycerol (pH 8.0)], re-suspended in 35 mL of the same buffer. The cell suspension was sonicated on ice. After centrifugation (13000 \times g for 40 min at 4°C), the supernatant was recovered and loaded on the Ni-NTA agarose chromatography (GE healthcare, Sweden) equilibrated with the same binding buffer. After extensive washing with binding buffer and washing buffer [50 mM Tris-HCl, 500 mM NaCl, 50 mM imidazole, 10% glycerol (pH 8.0)], His₆-Slr1588 protein was eluted from the resin with 8 mL of elution buffer [50 mM Tris-HCl, 500 mM NaCl, 500 mM imidazole, 10% glycerol (pH 8.0)] and further concentrated to about 1.0 mg/mL by ultrafiltration (Millipore membrane, 10 kDa cut-off size) according to the protocol provided by the manufacturer. The purity of the eluted His₆-Slr1588 protein was checked by SDS-PAGE electrophoresis.

Electrophoretic Mobility Shift Assays (EMSAs)

The EMSAs were performed as described before [39]. DNA fragments containing the different *Synechocystis* upstream regions of eight predicted target genes were amplified using genomic DNA of *Synechocystis* and primers listed in **Suppl. Table S1**. Probe labeling was achieved *via* a PCR reaction using Cy5-labelled primer (5'-AGCCAGTGGCGATAAG-3'), according to the method described by Tiffert *et al.* (2008) [40]. The amplified PCR products were purified using a QIAquick PCR Purification kit (QIAGEN, Germany). In each EMSA reaction, about 10 ng of labeled probes was incubated individually with various quantities of His₆-Slr1588 and 2 μ g of poly (dI-dC) (Roche, USA) at 25°C for 20 min in a final volume of 20 μ L of binding buffer containing 20 mM Tris-base (pH 7.9), 1 mM dithiothreitol (DTT), 10 mM MgCl₂, 0.2 mg/mL calf bovine serum albumin (BSA) and 5% glycerol. After incubation, protein-bound and free DNA were separated by electrophoresis on non-denaturing 6% polyacrylamide gels with 0.5 \times TBE running buffer at 10 V/cm and 4°C. For Cy5-labeled probe, gels were scanned directly by FujiFilm FLA-9000 (FUJIFILM, Japan). In order to quantify the probes, probe DNA concentrations were detected by ultraviolet spectrophotometer Nanodrop 2000 (Thermo

Cite this: DOI: 10.1039/c0xx00000x

www.rsc.org/xxxxxx

ARTICLE TYPE

Scientific, USA) at the wavelength of 260 nm.

Results and discussion

Slr1588 involves salt tolerance

To determine additional TCSTS genes that may be involved in salt tolerance, we subjected a library of gene deletion mutants for all 44 putative TCS response regulators constructed previously to a salt stress screening [41]. The mutants were grown in parallel with the wild-type *Synechocystis* in both normal BG11 liquid medium and the BG11 liquid medium supplemented with 4.0% NaCl (*w/v*). The analysis allowed identification of *slr1588* gene which may be involved in salt stress, as in the normal BG11 medium, no visible difference in terms of growth patterns between the wild-type control and the Δ *slr1588* mutant was observed (Fig. 1A); while in the BG11 medium supplemented with 4.0% NaCl, slower growth of the Δ *slr1588* mutant compared with the wild type strain was found (Fig. 1A). The increased sensitivity of the Δ *slr1588* mutant to salt stress was also observed on solid BG11 agar plate supplemented with 2.5% or 3.0% NaCl, when compared with the wild-type control (Fig. 1B).

So far no functional characterization has been conducted for the *slr1588* gene in the literature. Genomic context analysis showed no histidine kinase in the neighborhood of *slr1588*, suggesting it is an orphan response regulator gene (Fig. 2A). Protein domain analysis showed two distinct domains, a REC domain (CheY-homologous receiver domain) at N-terminus (*E* value 4.7e-39), and an EAL domain (putative diguanylate phosphodiesterase) close to C-terminus (*E* value 4.9e-133). In *E. coli* K-12, an anaerobic cyclic di-GMP phosphodiesterase YfgF with EAL domain was found involved in remodeling the cell surface and in the response to peroxide shock, with implications for integrating three global regulatory networks, *i.e.*, oxygen regulation, cyclic di-GMP signaling and the oxidative stress response [42]. Immediately downstream of *slr1588*, transcribed in the same direction, were two genes encoding a glucosylglycerol-phosphate phosphatase (*stpA* or *ggpP*, *slr0746*) and an ATP-binding subunit of an ABC-type osmolyte transporter (*ggtA*, *slr0747*), respectively; while immediately upstream of *slr1588*, transcribed in the opposite direction, was a gene encoding a large subunit of isopropylmalate isomerase (*leuC*, *sll1470*). The intergenic space between *slr1588* and downstream *slr0746* is 39 base-pairs (bp), while the intergenic space between *slr1588* and upstream *sll1470* is 229 bp. Interestingly, the glucosylglycerol-phosphate phosphatase of Slr0746 (GgpP) has been found involved in cyanobacterial osmotic response to salt shock as it is one of the key enzymes involved in synthesis of heteroside glucosylglycerol, which is

commonly found in moderate halotolerance cyanobacterial strains [43-46]. For the *slr0747* gene (*ggtA*) downstream of *slr0746*, previous studies have found that the *ggtA* insertion mutant in *Synechocystis* lost its glucosylglycerol uptake ability, but its salt tolerance did not change [47,48].

Considering that both *slr0746* and *slr0747* genes were involved synthesis and transport of the same compatible solute glucosylglycerol, and only small intergenic space was presented between them (*i.e.*, 138 bp) (Fig. 2A), we were tempted to determine whether they were transcribed as a single operon. The RT-PCR results showed that by using a primer set 2 covering both genes (Suppl. Table S1), a PCR fragment with the expected size can be amplified from the total RNA sample, suggesting *slr0746* and *slr0747* are indeed organized as a single operon (Fig. 2B).

Proteomic analysis of the *slr1588* gene deletion

To determine the differential cellular responses of *Synechocystis* to salt stress between the wild-type strain and the Δ *slr1588* mutant, and to further define the possible regulatory function of response regulator Slr1588, we performed a quantitative proteomic analysis of the wild-type control and the Δ *slr1588* mutant grown in BG11 medium supplemented with 4.0% NaCl. Two independent cultivations for both the wild-type control and the Δ *slr1588* mutant were established and the cells were collected by centrifugation (8,000 x *g* for 10 min at 4°C) at exponential phase (*i.e.*, 48 h) (Fig. 1). The purified protein samples were subjected to the iTRAQ - LC-MS/MS proteomic analysis using a Q Exactive high-performance mass spectrometer as described before [35,36]. After data filtering to eliminate low-scoring spectra, the qualified spectra were matched to 2,065 proteins, representing approximately 58% of the 3569 predicted proteins in the *Synechocystis* genome (Suppl. Table S2). Between two biological replicates of the wild type and the Δ *slr1588* mutant, four replicates of the proteomic analysis were established. As an index for protein identification confidence, for the 2,065 protein identified, more than 99.5% of the proteins (*i.e.*, 2,055) were detected in all four biological replicates, and only one protein was detected in only one of the four replicate samples (Suppl. Table S2). To access the repeatability of the quantitative proteomic analyses, we labeled and mixed two biological replicates of either the wild type or the Δ *slr1588* mutant samples directly for proteomic analysis. The difference was plotted verse the percentage of the proteins identified, and the results showed there were approximately 80% of the proteins with difference less than delta error of less than 0.3 and 0.4 for the wild type and the Δ *slr1588* mutant

replicates, respectively (Fig. 3A-B), suggesting that the biological noise was reasonably low. The relatively high proteome coverage and detection sensitivity may be due to: *i*) a SCX fraction step was applied to the peptide samples and twenty fractions were collected and subjected to the proteomic analysis, which has increased the protein coverage for more than 30% compared to the similar samples without a SCX fraction step [29,30]; *ii*) a Q-EXACTIVE hybrid quadrupole-Orbitrap high-performance mass spectrometer used in this study allowed for 10 MS/MS spectra per second to be acquired, resulting in an unprecedented number of protein identifications; and it acquires the precursor and product ion masses at high resolution [35,36].

Global effects of Slr1588

Using a cutoff of 2.0-fold change and a statistical significance *p*-value less than 0.05, we determined that between the *Δslr1588* mutant and the wild type grown under 4.0% NaCl, 113 and 127 unique proteins were up- and down-regulated, respectively (Suppl. Table S3 and S4). Functional category analysis showed that a wide range of cellular functions were differentially in the *Δslr1588* mutant grown under salt stress, suggesting that the *slr1588* deletion has caused significant cellular responses, although quite likely as indirect effects of the gene deletion. One notable feature is the down-regulation of proteins related to transporting functions (*i.e.*, SII0507, SII0689, SII1600, Slr0615, Slr0798, Slr0875, Slr0944, Slr1295, Slr1392, Slr1512) (Suppl. Table S4). Among them, SII0689 has been suggested as important for salt tolerance and essential for growth under the various conditions [49]; Slr0875 (SyMscL) was found contributing to the adaptation to hypoosmotic stress [50]; Slr1295 (FutA1) exhibited the highest enhancement during salt stress, and play roles in protection of photosystem II under iron deficiency [51]; and Slr1512 (SbtA) was essential to sodium-dependent bicarbonate transport in *Synechocystis* [52]. Another notable feature is the down-regulation of proteins known to be important to intracellular metal homeostasis, including Slr0945 of an arsenical resistance protein ArsH homolog and Slr0946 of an arsenate reductase involved in cadmium metabolism [53,54], Slr0798 of a zinc-transporting P-type ATPase (zinc efflux pump) involved in zinc metabolism [55], SII0789 and SII0790 of a two-component signal system involved in copper metabolism [56]. Although the details still unclear, it is speculative that stress resistance mechanisms that these protein involved can also be used against salt stress [57].

Meanwhile, up-regulation of many ribosomal proteins (*i.e.*, *sll1800*, *sll1803*, *sll1804*, *sll1808*, *sll1810*, *sll1811*, *sll1813*, *sll1816*, *sll1822*, *slr0628*, *slr0744*, *slr0974*, *ssl1784*, *ssl2233*, *ssl3437*, *ssl3441*, *ssr0482*, *ssr1399*, *ssr2799*), and protein translation initiation factor IF-1, IF-2 and IF3 (*i.e.*, *ssl3441*, *slr0744*, *slr0974*) was observed in the *Δslr1588* mutant grown under salt stress. In addition, up-regulation of several photosynthesis-related proteins,

including Slr0171 of a photosystem I assembly related protein Ycf37, Slr0343 of a cytochrome b6-f complex subunit 4, Slr0506 of a light-dependent NADPH-protochlorophyllide oxidoreductase, Slr0772 of a light-independent protochlorophyllide reductase subunit ChlB, Slr1311 of a photosystem II D1 protein, Slr1739 of a photosystem II 13 kDa protein homolog, Slr2033 of a membrane-associated rubredoxin essential for photosystem I assembly, Smr0010 of a cytochrome b6-f complex subunit 5, and Ssl2598 of a photosystem II PsbH protein, was also observed in the *Δslr1588* mutant grown under salt stress. Although it is still unclear how Slr1588 regulated the proteins, the up-regulation of protein synthesis and photosynthesis has been reported for *Synechocystis* under salt stress [58].

A proteomic analysis of the plasma membrane from a salt-responsive histidine kinase (*hik33*)-knockout mutant (Δ Hik33) under normal and salt-stress conditions was reported recently [59]. Using 2D-DIGE followed by mass spectrometry analysis, more than two dozens proteins were identified as differentially expressed proteins in Δ Hik33 mutant cells under salt stress, including a response regulator Rre13 (*slr2024*). However, when compared with the proteomic results of the *Δslr1588* mutant grown under salt stress, only one protein, Slr1919 of ABC1-like transporter, was found sharing the same patterns of regulation, and was up-regulated in both Δ Hik33 and *Δslr1588* mutants. The different responses for the Δ Hik33 and the *Δslr1588* mutants under salt stress suggested that they could be independently operating, in response to different signals related to salt stress.

Differential expression of proteins involved in compatible solute synthesis in the *Δslr1588* mutant

Compatible solutes are a functional group of small, highly soluble organic molecules that accumulate during the acclimation of bacteria to adverse environmental conditions, particularly to salt and drought stress [60]. In photosynthetic cyanobacteria, sucrose, trehalose, glucosylglycerol and glycine betaine have been identified as major compatible solutes, among which glucosylglycerol and sucrose were found as common compatible solutes in *Synechocystis* [60]. According to early researches, the corresponding biosynthetic pathways for glucosylglycerol and sucrose have been established [60]. The glucosylglycerol biosynthetic pathway included a step that is carried out by the glucosylglycerol-phosphate synthase (GgpS, SII1566) and another step that is catalyzed by the glucosylglycerol-phosphate phosphatase (GgpP, Slr0746) [60]. While sucrose synthesis involves a sucrose-phosphate synthase (SpsA, SII0045) and sucrose-phosphatase (Spp, Slr0953) in *Synechocystis* [61,62], in which sucrose-phosphate phosphatase (Spp) catalyzes the hydrolysis of sucrose 6-phosphate to Sucrose, and SpsA is a large protein of approximately 80 kDa with an N-terminal domain that contains all of the features required for Sps activity and with a C-terminal domain of about 20 kDa that shares

Cite this: DOI: 10.1039/c0xx00000x

www.rsc.org/xxxxxx

ARTICLE TYPE

similarities with Spp [60]. Between the two types of compatible solutes, glucosylglycerol and sucrose, it has been reported that cyanobacterial mutants with inactivated *ggpS* genes and salt-sensitive phenotype had increased content of sucrose [44, 60,63], suggesting that cyanobacteria can achieve protection of cells against salt by balancing the concentration of these two types of important compatible solutes.

According to the phenotypic analysis of salt tolerance and the gene organization, we proposed that response regulator Slr1588 may be involved in glucosylglycerol synthesis directly in *Synechocystis*. To prove the hypothesis, we determined the differentially expressed proteins between the Δ *slr1588* mutant and the wild type under salt stress. Expression levels of proteins known involved in compatible solute synthesis were listed in **Table 1**. The proteomic data showed that the GgpP (Slr0746) protein was up-regulated 3.37 folds in the Δ *slr1588* mutant under salt stress, suggesting that Slr1588 may be functional as a negative regulator for expression of the *ggpP* gene; in addition, GgtA (Slr0747) protein was also up-regulated by 1.64 folds, suggesting that the expression of the ABC-type osmolyte transporter was also negatively regulated directly by Slr1588, consistent with the above conclusion that *slr0746* and *slr0747* were organization in a single operon (**Fig. 2B**). Interestingly, the proteomic analysis also showed that in the Δ *slr1588* mutant glucosylglycerol-phosphate synthase (GgpS, Sll1566) was up-regulated 2.39-fold and 3.40-fold in two biological replicates, respectively; in addition, Sll1085 of glycerol 3-phosphate dehydrogenase (GlpD) whose encoding gene is located immediate downstream of *sll1566* and is also involved in glucosylglycerol metabolism, was also up-regulated 2.17-3.89 folds in three of the four biological replicates, suggesting that Slr1588 may also negatively regulate expression of these two genes. Early study has identified a regulator protein GgpR (Ssl3076) acts to repress *ggpS* and *glpD* expression under salt stress conditions, as expression levels of *ggpS* and *glpD* were increased in the Δ *ggpR* mutant; however, the expression of *ggpP* (*slr0746*) was not affected in the Δ *ggpR* mutant [64], suggesting *ggpS* and *ggpP* were subjected to different regulatory controls. Our proteomic results were consistent with this early discovery that both GgpS and GlpD were up-regulated by the *slr1588* deletion; in addition, our data showed that Slr1588 might also negatively regulate the expression of both *ggpS* and *ggpP*, suggesting it may be an independent regulatory mechanism from the GgpR (Ssl3076). The up-regulation of Slr0746, Slr0747, Sll1566 and Sll1085 was also verified by RT-qPCR at transcriptional level (**Table 1**).

Our proteomic analysis showed sucrose-phosphate synthase (SpsA, Sll0045) was up-regulated in the Δ *slr1588* mutant under salt stress. Although we were not able to identify another key sucrose biosynthesis enzymes, sucrose-phosphatase (Spp, Slr0953) (**Suppl. Table 2**), the proteomic analysis showed that Slr0952 whose encoding gene is located immediately upstream of *slr0953* and encodes a fructose-1,6-bisphosphatase was up-regulated (**Table 1**). Fructose-1,6-bisphosphatase catalyzes the conversion of fructose-1,6-bisphosphate to fructose 6-phosphate, was suggested recently as a key step in photosynthetic sucrose synthesis in *Arabidopsis* plants [65]. Up-regulation of both glucosylglycerol and sucrose biosynthesis in the Δ *slr1588* mutant under salt stress is interesting, which is different from the early results that *ggpS* gene mutation has increased the cellular content of sucrose [45,61,64], suggesting that cyanobacteria can also achieve protection of cells against salt stress by enhancing concentration of both types of important compatible solutes at the same time. The up-regulation of Sll0045 and Slr0952 was also verified by RT-PCR at transcriptional level (**Table 1**). In addition, along with up-regulation of proteins directly involved in sucrose synthesis, the proteomic analysis showed that other proteins relevant to sucrose biosynthesis, such as fructose-bisphosphate aldolase (Sll0018), putative glucose dehydrogenase (Slr1608) and UDP-glucose 4-epimerase (Slr1617) were also up-regulated (**Table 1**), which may further improve the carbon flux into sucrose biosynthesis.

Direct binding of Slr1588 to the upstream regions of genes relevant to biosynthesis of compatible solutes

According to the proteomic analysis, we proposed that the Slr1588 response regulator might serve as a repressor and directly bind to the upstream region of genes involved in the synthesis of glucosylglycerol and sucrose. To prove this hypothesis, we conducted an EMSA analysis using the purified His₆-Slr1588 and putative promoter regions of 7 coding genes known to be involved in biosynthesis of compatible solutes, glucosylglycerol and sucrose (*i.e.*, *sll0045*, *sll1085*, *sll1566*, *slr0746*, *slr0747*, *slr0952*, *slr0953*), and the Na⁺/H⁺ antiporter gene *sll0689* that was previously found essential for salt tolerance [49] (**Table 1, Suppl. Table S3**). The *slr1588* gene was expressed in *E. coli* and his-tagged protein was purified to >90% pure as judged by SDS-PAGE (**Fig. 4A**). In the EMSAs, probes containing the corresponding upstream regions of selected genes were PCR amplified and labeled for binding evaluation. As shown in **Fig. 4B**, clear gel-shift pattern of the purified His₆-Slr1588 protein was observed for *sll1566* encoding a glucosylglycerol-

phosphate synthase (GgpS) and *sll0045* encoding a sucrose-phosphate synthase (SpsA). However, no convincing direct binding was observed for the reminding 6 target genes under the testing conditions. Non-binding of His₆-Slr1588 protein and putative promoter regions of *slr0746* and *slr0942* was presented as a negative control in **Fig. 4B**. For *sll0045*, two binding bands were observed, which was probably due to discrete regions bound by Slr1588 locating in the amplified promoter region, as similar phenomena were also reported for a regulator protein AtrA in *Streptomyces coelicolor* [66]. Considering His₆-Slr1588 bound *sll1566* and *sll0045* genes were both up-regulated in the Δ *slr1588* mutant grown under salt stress, we proposed that the Slr1588 response regulator functioned negatively on the expression of these target genes.

Conclusions

Although several TCSTS and other regulatory genes have been previously identified related to salt tolerance in *Synechocystis* [23-25, 67-69], the studies indicated that additional TCSTS or other type of regulatory genes might be still needed to execute the complex response related to salt stress [24]. In this study, by screening the knockout mutant library of all response regulator genes, we found that a novel orphan response regulator Slr1588 involved salt tolerance in *Synechocystis*. To decipher its regulatory mechanism, a high performance Q-EXACTIVE hybrid quadrupole-Orbitrap mass spectrometer was used to perform comparative proteomic analysis of the Δ *slr1588* mutant and the wild-type control under 4.0% NaCl. The results showed that a wide range of cellular functions could be affected by *slr1588* deletion, although most of them are likely secondary effects. To further define targets of Slr1588, an EMSAs experiments were conducted and the results showed that the purified his-tagged Slr1588 might be able to bind *in vitro* directly to the upstream regions of *sll0045* required for sucrose biosynthesis, and *sll1566* (*ggpS*) required for glucosylglycerol biosynthesis. In addition, the study showed that the regulatory pathway mediated by Slr1588 might be independent from that of the regulator Ssl3076. The scheme of the Slr1588 regulatory network related to salt stress was presented in **Fig. 5**, showing that the orphan two-component response regulator Slr1588 involves salt tolerance by directly regulating glucosylglycerol and sucrose synthesis in photosynthetic *Synechocystis*. The study revealed a novel salt-tolerant regulatory mechanism mediated by Slr1588, and also provided a proteomic description of the possible Slr1588 regulon in *Synechocystis*.

Acknowledgements

The research was supported by grants from National Basic Research Program of China ("973" program, project No. 2011CBA00803, No. 2014CB745101 and No. 2012CB721101), National High-tech R&D Program ("863" program, project No.

2012AA02A707), and the Tianjin Municipal Science and Technology Commission (No. 12HZGJHZ01000). The authors would also like to thank Tianjin University and the "985 Project" of Ministry of Education for their generous supports in establishing the research laboratory.

References

1. J. B. Stock, A. J. Ninfa, and A. M. Stock, *Microbiol. Rev.*, 1989, **53**, 450-490.
2. J. A. Hoch, *Curr. Opin. Microbiol.*, 2000, **3**, 165-170.
3. E. J. Capra, and M. T. Laub, *Annu. Rev. Microbiol.*, 2012, **66**, 325-347.
4. K. Jung, L. Fried, S. Behr, and R. Heermann, *Curr. Opin. Microbiol.*, 2012, **15**, 118-124.
5. A. I. Podgornaia, and M. T. Laub, *Curr. Opin. Microbiol.*, 2013, **16**, 156-162.
6. M. K. Ashby, and J. Houmard, *Microbiol. Mol. Biol. Rev.*, 2006, **70**, 472-509.
7. M. Hagemann, *FEMS Microbiol. Rev.*, 2011, **35**, 87-123.
8. F. Kunst, and G. Rapoport, *J. Bacteriol.*, 1995, **177**, 2403-2407.
9. J. Nogales, R. Campos, H. BenAbdelkhalik, J. Olivares, C. Lluch, and J. Sanjuan, *Mol. Plant Microbe Interact.*, 2002, **15**, 225-232.
10. L. Brondsted, B. H. Kallipolitis, H. Ingmer, and S. Knochel, *FEMS Microbiol. Lett.*, 2003, **219**, 233-239.
11. J. Rodriguez-Moya, M. Argandona, M. Reina-Bueno, J. J. Nieto, F. Iglesias-Guerra, M. Jebbar, and C. Vargas, *BMC Microbiol.*, 2010, **10**, 256.
12. G. Jubelin, A. Vianney, C. Beloin, J. M. Ghigo, J. C. Lazzaroni, P. Lejeune, and C. Dorel, *J. Bacteriol.*, 2005, **187**, 2038-2049.
13. R. Heermann, A. Weber, B. Mayer, M. Ott, E. Hauser, G. Gabriel, T. Pirch, and K. Jung, *J. Mol. Biol.*, 2009, **386**, 134-148.
14. S. Puranik, S. Shaligram, V. Paliwal, D. V. Raje, A. Kapley, and H. J. Purohit, *Bioresour. Technol.*, 2012, **121**, 282-289.
15. L. C. Wang, L. K. Morgan, P. Godakumbura, L. J. Kenney, and G. S. Anand, *EMBO J.*, 2012, **31**, 2648-2659.
16. D. J. W. Lane, A. R. Beaumont, and J. R. Jr Hunter, *Limnol. Oceanogr.*, 1994, **39**, 169-175.
17. E. Blumwald, R. J. Mehlhorn, and L. Packer, *Plant Physiol.*, 1983, **73**, 377-380.
18. R. H. Reed, S. R. C. Warr, D. L. Richardson, D. J. Moore, and W. D. P. Stewart, *FEMS Microbiol. Lett.*, 1985, **28**, 225-229.
19. S. Fulda, S. Mikkat, F. Huang, J. Huckauf, K. Marin, B. Norling, and M. Hagemann, *Proteomics*, 2006, **6**, 2733-2745.
20. N. Matsuda, H. Kobayashi, H. Katoh, T. Ogawa, L. Futatsugi, T. Nakamura, E. P. Bakker, and N. Uozumi, *J. Biol. Chem.*, 2004, **279**, 54952-54962.
21. M. Hagemann, S. Fulda, and H. Schubert, *Curr. Microbiol.*, 1994, **28**, 201-207.
22. K. Marin, Y. Kanesaki, D. A. Los, N. Murata, I. Suzuki, and M. Hagemann, *Plant Physiol.*, 2004, **136**, 3290-3300.
23. S. H. Schwartz, T. A. Black, K. Jager, J. M. Panoff, and C. P. Wolk, *J. Bacteriol.*, 1998, **180**, 6332-6337.
24. K. Marin, I. Suzuki, K. Yamaguchi, K. Ribbeck, H. Yamamoto, Y. Kanesaki, M. Hagemann, and N. Murata, *Proc. Natl. Acad. Sci. U.S.A.*, 2003, **100**, 9061-9066.
25. M. A. Shoumskaya, K. Paitoonrangsarid, Y. Kanesaki, D. A. Los, V. V. Zinchenko, M. Tanticharoen, I. Suzuki, and N. Murata, *J. Biol. Chem.*, 2005, **280**, 21531-21538.

Cite this: DOI: 10.1039/c0xx00000x

www.rsc.org/xxxxxx

ARTICLE TYPE

26. B. Wang, J. Wang, W. Zhang, and D. R. Meldrum, *Front. Microbiol.*, 2012, **3**, 344.
27. B. Wang, S. Pugh, D. R. Nielsen, W. Zhang, and D. R. Meldrum, *Metab. Eng.*, 2013, **16**, 68-77.
- 870 28. M. J. Dunlop, *Biotechnol. Biofuels*, 2011, **4**, 32.
29. J. Qiao, J. Wang, L. Chen, X. Tian, S. Huang, X. Ren, and W. Zhang, *J. Proteome Res.*, 2012, **11**, 5286-5300.
30. X. Tian, L. Chen, J. Wang, J. Qiao, and W. Zhang, *J. Proteomics*, 2013, **78**, 326-345.
- 875 31. J. Wang, L. Chen, S. Huang, J. Liu, X. Ren, X. Tian, J. Qiao, and W. Zhang, *Biotechnol. Biofuels*, 2012, **5**, 89.
32. H. Alper, and G. Stephanopoulos, *Metab. Eng.*, 2007, **9**, 258-267.
- 880 33. H. Alper, J. Moxley, E. Nevoigt, G. R. Fink, and G. Stephanopoulos, *Science*, 2006, **314**, 1565-1568.
34. H. L. Wang, B. L. Postier, and R. L. Biotechniques, 2002, **33**, 26, 28, 30.
35. A. Michalski, E. Damoc, J. P. Hauschild, O. Lange, A. Wiegand, A. Makarov, N. Nagaraj, J. Cox, M. Mann, and S. Horning, 2011, **10**, M111-M11015.
- 885 36. C. D. Kelstrup, C. Young, R. Lavallee, M. L. Nielsen, and J. V. Olsen, *J. Proteome Res.*, 2012, **11**, 3487-3497.
37. T. Kaneko, Y. Nakamura, S. Sasamoto, A. Watanabe, M. Kohara, M. Matsumoto, S. Shimpō, M. Yamada, and S. Tabata, *DNA Res.*, 2003, **10**, 221-228.
- 890 38. N. Kloft, G. Rasch, and K. Forchhammer, 2005, **151**, 1275-1283.
39. Z. Yu, H. Zhu, F. Dang, W. Zhang, Z. Qin, S. Yang, H. Tan, Y. Lu, and W. Jiang, *Mol. Microbiol.*, 2012, **85**, 535-556.
- 895 40. Y. Tiffert, P. Supra, R. Wurm, W. Wohlleben, R. Wagner, and J. Reuther, *Mol. Microbiol.*, 2008, **67**, 861-880.
- 900 41. L. Chen, Y. Zhu, Z. Song, J. Wang, and W. Zhang, *Mol. Cell Proteomics*, Submitted.
42. M. M. Lacey, J. D. Partridge, and J. Green, 2010, **156**, 2873-2886.
43. M. Hagemann, A. Schoor, R. Jeanjean, E. Zuther, and F. Joset, *J. Bacteriol.*, 1997, **179**, 1727-1733.
- 905 44. K. Marin, E. Zuther, T. Kerstan, A. Kunert, and M. Hagemann, *J. Bacteriol.*, 1998, **180**, 4843-4849.
45. S. Klahn, A. Hohne, E. Simon, and M. Hagemann, *J. Bacteriol.*, 2010, **192**, 4403-4412.
- 910 46. X. Mao, V. Olman, R. Stuart, I. T. Paulsen, B. Palenik, and Y. Xu, *BMC Genomics*, 2010, **11**, 291.
47. M. Hagemann, S. Richter, and S. Mikkat, *J. Bacteriol.*, 1997, **179**, 714-720.
48. K. Marin, Y. Kanesaki, D. A. Los, N. Murata, I. Suzuki, and M. Hagemann, *Plant Physiol.*, 2004, **136**, 3290-3300.
- 915 49. H. L. Wang, B. L. Postier, and R. L. Burnap, *Mol. Microbiol.*, 2002, **44**, 1493-1506.
50. K. Nanatani, T. Shijuku, M. Akai, Y. Yukutake, M. Yasui, S. Hamamoto, K. Onai, M. Morishita, M. Ishiura, and N. Uozumi, *Channels (Austin)*, 2013, **7**, 238-242.
- 920 51. F. Huang, S. Fulda, M. Hagemann, and B. Norling, *Proteomics*, **6**, 910-920.
52. M. Shibata, H. Katoh, M. Sonoda, H. Ohkawa, M. Shimoyama, H. Fukuzawa, A. Kaplan, and T. Ogawa, *J. Biol. Chem.*, 2002, **277**, 18658-18664.
- 925 53. R. Li, J. D. Haile, and P. J. Kennelly, *J. Bacteriol.*, 2003, **185**, 6780-6789.
54. L. Lopez-Maury, F. J. Florencio, and J. C. Reyes, *J. Bacteriol.*, 2003, **185**, 5363-5371.
- 930 55. C. Thelwell, N. J. Robinson, and J. S. Turner-Cavet, *Proc. Natl. Acad. Sci. U.S.A.*, 1998, **95**, 10728-10733.
56. J. Giner-Lamia, L. Lopez-Maury, J. C. Reyes, and F. J. Florencio, *Plant Physiol.*, 2012, **159**, 1806-1818.
57. T. Jittawuttipoka, M. Planchon, O. Spalla, K. Benzerara, F. Guyot, C. Cassier-Chauvat, and F. Chauvat, *PLoS One*, 2013, **8**, e55564.
- 935 58. J. Pandhal, J. Noirel, P. C. Wright, and C. A. Biggs, *Saline Systems*, 2009, **5**, 8.
59. T. Li, H. M. Yang, S. X. Cui, I. Suzuki, L. F. Zhang, L. Li, T. T. Bo, J. Wang, N. Murata, and F. Huang, *J. Proteome Res.*, 2012, **11**, 502-514.
- 940 60. S. Klahn, and M. Hagemann, *Environ. Microbiol.*, 2011, **13**, 551-562.
61. L. Curatti, E. Folco, P. Desplats, G. Abratti, V. Limones, L. Herrera-Estrella, and G. Salerno, *J. Bacteriol.*, 1998, **180**, 6776-6779.
62. J. E. Lunn, *Plant Physiol.*, 2002, **128**, 1490-1500.
63. F. Engelbrecht, K. Marin, and M. Hagemann, *Appl. Environ. Microbiol.*, 1999, **65**, 4822-4829.
- 950 64. S. Klahn, A. Hohne, E. Simon, and M. Hagemann, *J. Bacteriol.*, 2010, **192**, 4403-4412.
65. M. H. Cho, A. Jang, S. H. Bhoo, J. S. Jeon, and T. R. Hahn, *Photosynth. Res.*, 2012, **111**, 261-268.
66. G. C. Uguru, K. E. Stephens, J. A. Stead, J. E. Towle, S. Baumberg, and K. J. McDowall, *Mol. Microbiol.*, 2005, **58**, 131-150.
- 955 67. C. Liang, X. Zhang, X. Chi, X. Guan, Y. Li, S. Qin, and H.B. Shao, *PLoS One*, 2011, **6**, e18718.
68. T. Tyystjärvi, T. Huokko, S. Rantamäki, and E. Tyystjärvi, *PLoS One*, 2013, **8**, e63020.
- 960 69. Y. Wang, and X. Xu, *FEBS Lett.* 2013, **587**, 1446-1451.

Figure Legends

970 **Fig. 1: Growth of the wild type and the mutant $\Delta slr1588$ in BG11 medium with or without salt.** A) BG11 liquid medium was supplemented with 4.0% NaCl. B) BG11 agar plate was supplemented with 2.5% or 3.0% NaCl.

Fig. 2: A) Organization of *slr1588* and its nearby genes in the chromosome; B) RT-PCR analysis of *slr0746-slr0747* transcript. Lane M: DNA markers. Lane 1, 2 or 3: RT-PCR product using corresponding primer set 1, 2 or 3 as indicated in panel A).

975 **Fig. 3: Repeatability of proteomic data between biological replicates.** A) the wild type; B) the $\Delta slr1588$ mutant.

Fig. 4: EMSA of the interaction of Slr1588 response regulator with several putative promoter regions. A) SDS-PAGE analysis of expression and purification of His₆-Slr1588 in *E. coli* BL21(DE3). Lane 1: the crude extract of *E. coli* BL21 (DE3) harboring pET46-1588 without being induced by IPTG; Lanes 2 and 3: the supernatant and the precipitate fractions of *E. coli* BL21(DE3) harboring pET46-1588 induced by IPTG at a final concentration of 0.2 mM at 18 °C overnight; Lane 4: the purified His₆-Slr1588 protein; Lane M: protein markers; B) EMSAs of the promoter regions of *slr1566*, *slr0045*, *slr0746*, and *slr0952* with purified His₆-Slr1588. Lanes 1, 2, 3, 4, 5 and 6 contain 0, 2.4, 4.8, 7.2, 9.6 and 12.0 μM of His₆-Slr1588 respectively and 10 ng each of 5'-cy5-labelled probes was added in each of the EMSAs reactions.

985 **Fig. 5: Scheme of the compatible solute synthesis regulatory network mediated by Slr1588.** Green lines indicated regulation according to proteomic analysis and EMSA evidences of direct bindings. Red lines indicated regulation according to only proteomic analysis, while no EMSA evidences of direct bindings.

Supplementary materials available online:

Suppl. Table S1: Primers used in this study.

990 **Suppl. Table S2: All proteomes detected in the proteomic study.**

Suppl. Table S3: Proteins up-regulated in the $\Delta slr1588$ mutant upon salt exposure.

Suppl. Table S4: Proteins down-regulated in the $\Delta slr1588$ mutant upon salt exposure.

995

Cite this: DOI: 10.1039/c0xx00000x

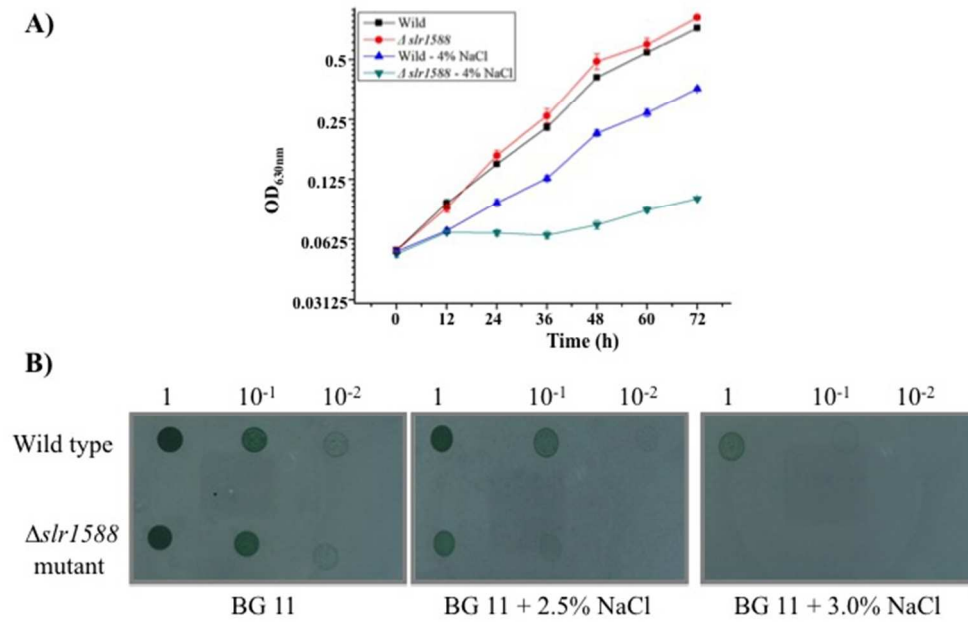
www.rsc.org/xxxxxx

ARTICLE TYPE

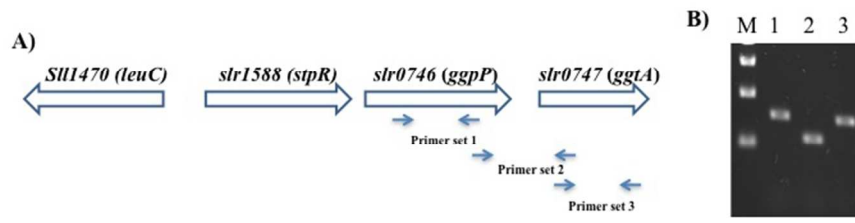
Table 1: Up-regulated compatible solute synthesis related proteins in the $\Delta slr1588$ mutant upon salt exposure.

Protein ID	Slr1588-r1 vs. Control-r1		Slr1588-r2 vs. Control-r1		Slr1588-r1 vs. Control-r2		Slr1588-r2 vs. Control-r2		RT-PCR ratio	Description
	Ratio	Sequence coverage								
Slr1566					3.40	34.30	2.39	34.30	1.43 ± 0.060	Glucosylglycerolphosphate synthase
Slr0746			3.37	15.40					1.32 ± 0.008	Glucosylglycerolphosphate phosphatase
Slr0045	1.69	4.60			3.77	4.60	1.53	4.60	2.06 ± 0.288	Sucrose phosphate synthase
Slr1085			2.17	32.60	3.89	32.60	2.54	32.60	2.18 ± 0.126	Glycerol-3-phosphate dehydrogenase
Slr0952					1.95	51.00			1.45 ± 0.055	Fructose-1,6-bisphosphatase
Slr0747	1.64	19.50							1.40 ± 0.107	Glucosylglycerol transport system ATP-binding protein

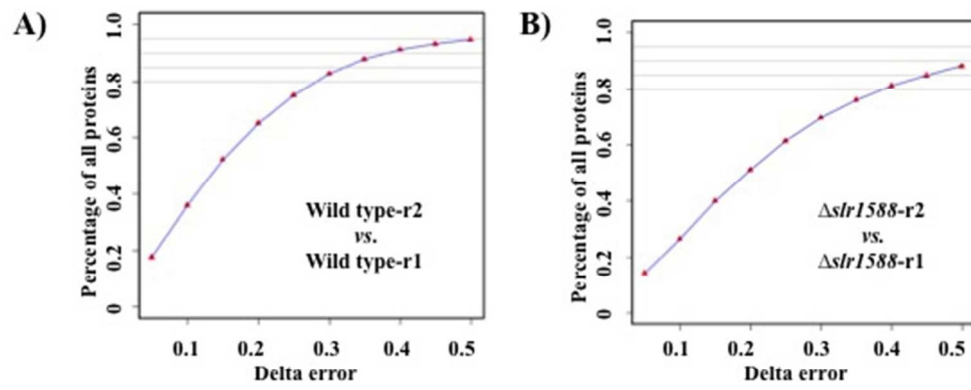
1000



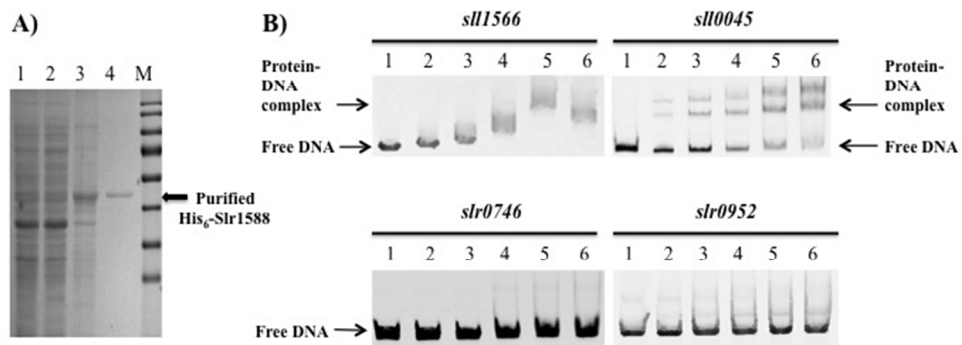
249x156mm (72 x 72 DPI)



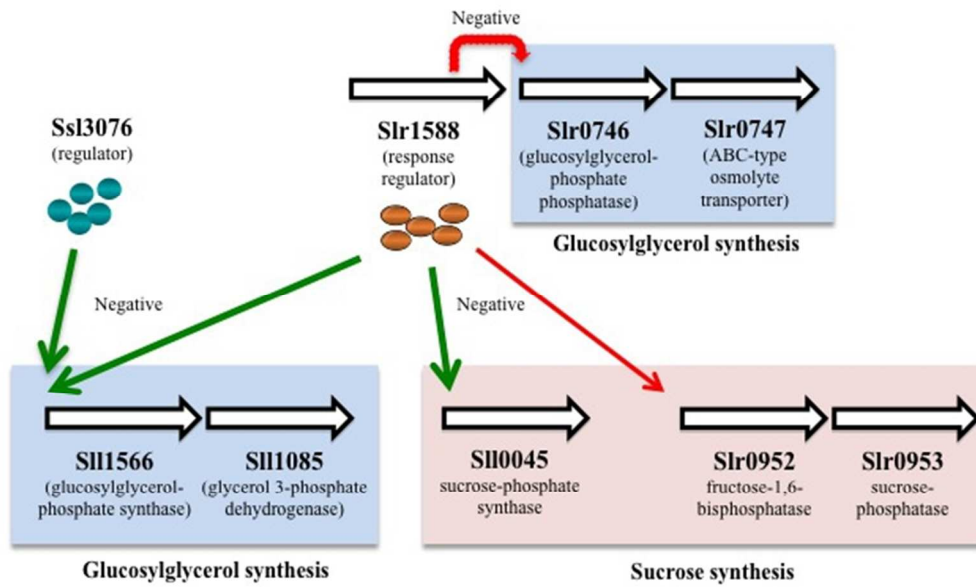
276x61mm (72 x 72 DPI)



196x91mm (72 x 72 DPI)



249x86mm (72 x 72 DPI)



224x132mm (72 x 72 DPI)